

Phonon spectra of $\text{Pd}_x\text{Fe}_{1-x}$ alloys with transferable force constants

This article has been downloaded from IOPscience. Please scroll down to see the full text article.

2009 J. Phys.: Condens. Matter 21 395401

(<http://iopscience.iop.org/0953-8984/21/39/395401>)

View [the table of contents for this issue](#), or go to the [journal homepage](#) for more

Download details:

IP Address: 129.252.86.83

The article was downloaded on 30/05/2010 at 05:27

Please note that [terms and conditions apply](#).

Phonon spectra of $\text{Pd}_x\text{Fe}_{1-x}$ alloys with transferable force constants

Biswanath Dutta and Subhradip Ghosh

Department of Physics, Indian Institute of Technology Guwahati, Guwahati, Assam 781039, India

E-mail: b.dutta@iitg.ernet.in

Received 29 May 2009, in final form 10 August 2009

Published 8 September 2009

Online at stacks.iop.org/JPhysCM/21/395401

Abstract

The transferable force constant model of van de Walle *et al* (2002 *Rev. Mod. Phys.* **74** 11) has been combined with the itinerant coherent potential approximation to calculate the complete phonon spectra and elastic constants in the magnetic type-II alloy $\text{Pd}_x\text{Fe}_{1-x}$ across the concentration range. The calculated dispersion curves and elastic constants agree very well with the experiments. We discuss the results in the light of the behavior of inter-atomic force constants between various pairs of chemical species. The results demonstrate that the combination of the transferable force constant model and the ICPA method for configuration averaging serve as an efficient and reliable first-principles-based tool to compute the phonon spectra for disordered alloys at any arbitrary concentration.

1. Introduction

The study of lattice vibrations in the presence of substitutional disorder is one of the most fascinating areas of condensed matter physics. A wide variety of physical properties of solids [1] depend on their lattice-dynamical behavior which makes the investigation of the governing physics of these systems intriguing. The technological importance of these alloys, on the other hand, has added an extra dimension and provided the necessary momentum towards the research and analysis of these systems. As far as experimental realization is concerned, a huge array of data is available [2–9] at both stoichiometric and off-stoichiometric compositions, exploring the effect of lattice dynamics on various material properties of the system. The theoretical study, on the other hand, has got the necessary boost only recently with the advent of the ‘itinerant coherent potential approximation’ (ICPA) [10] and the state-of-the-art first-principles density functional theory (DFT) [11, 12]-based ‘density functional perturbation theory’ (DFPT) [13]. Based upon the *augmented space formalism* [14], the ICPA is a mean-field-based cluster generalization of the single-site coherent potential approximation (CPA) [15]. In combination with DFPT, this ICPA method has been tested on a number of systems [16–18] and is found to produce satisfactory results on most occasions. However, as mentioned in the original formalism, the ICPA is heavily dependent upon the accuracy of the inter-atomic force constants. Due

to the random chemical environment around each atom in a substitutionally disordered alloy, the force constants corresponding to A–A, B–B and A–B pairs in an A_xB_{1-x} alloy are different from those in the ordered alloy and in no way resemble the force constants in a completely ordered environment. In order to have significant accuracy in calculated phonon properties one should, therefore, have accurate information on force constants corresponding to various pairs of chemical species. The quest, thus, is to look for a reliable source of inter-atomic force constants in random alloys. The most trustworthy source available in this regard are the first-principles electronic structure methods. However, state-of-the-art *ab initio* calculations always assume some degree of translational symmetry in disordered systems. For calculations of properties in disordered alloys through first-principles techniques, one has to construct either a large supercell or, as is done in conventional alloy theory, a cluster expansion [19] has to be fitted to the ground state energies of a large number of ordered states. While the calculation for a given ordered structure is a relatively routine task with modern first-principles electronic structure codes, this procedure has to be repeated for many configurations in order to properly fit a cluster expansion, which makes the whole procedure computationally demanding. Similar is the case for the supercell technique. For calculation of phonon excitations, the computational cost rises even further. Thus, in spite of having a suitable self-consistent analytical technique to

perform the required averaging over various configurations in the disordered systems, the calculations of the phonon spectrum in random alloys were rather limited because of these practical difficulties.

Recently, a new idea has been proposed to alleviate the problem of heavy computational cost. In *ab initio* calculations, most of the computational burden comes from the calculation of the force constant tensors. It would thus be extremely helpful if the force constants determined in one structure could be used to predict force constants in another structure. However, it was observed that the force constants obtained from one structure are not directly transferable to another structure [20, 21]. Nevertheless, a simple modification of the transferable force constant approach yields substantial improvements in precision. Initially defined for the transferability of force constants for a particular pair type [20], van de Walle and Ceder have recently introduced the idea of using bond-length-dependent transferable force constants [22–24]. Their calculations on a number of systems [21–24] had revealed that most of the variation in the stiffness of a given chemical bond across different structures can be explained by changes in bond length alone, which suggests that the force constant versus bond length relationships exhibit better transferability than force constants themselves. This approach provides a very simplistic and computationally feasible way to determine the force constants, as the force constant versus bond length relationships can be determined from a relatively small number of first-principles calculations on select configurations and then can be transferred to determine the force constants for other atomic configurations, once the relevant bond lengths are known.

In all the calculations with this ‘bond stiffness versus bond length’ approach the focus has been on calculations of vibrational entropy contributions in the context of relative stability of various ordered and disordered phases. The complete phonon spectra and related material properties, like the elastic constants, were never calculated using this approach. The reliability of the transferable force constant model (TFC) cannot be completely satisfactory unless one computes the complete phonon spectra. This is because of the fact that, in cases of the calculation of vibrational entropies or their differences, the key quantity is the vibrational densities of states, an integrated quantity which therefore may average out errors through the integration process. The phonon frequencies, on the other hand, would reflect the errors due to the approximation in a proper way. Another noteworthy point is that the TFC model has never been applied to magnetic alloys. It is a well-known fact that, for type-II alloys like FePt and FePd, where the constituents, in spite of crystallizing in different structures in their respective ground states, form a single solid solution upon alloying. These alloys at compositions near the invar region exhibit an interplay of magnetism and lattice dynamics [25, 26]. The computation and understanding of phonon spectra in these alloys is, thus, necessary to understand the microscopic nature of magnetism–phonon interaction in these technologically important systems.

In this paper, we compute the phonon spectra and elastic constants for the magnetic type-II alloy $\text{Pd}_x\text{Fe}_{1-x}$ with

$x = 0.96, 0.9, 0.5$ and 0.28 . The reasons for choosing these alloys are threefold:

- (i) to check the validity of the TFC model in the context of a magnetic type-II alloy,
- (ii) to check whether the combination of the TFC model for extraction of accurate force constants in a random alloy and the ICPA method to perform the configuration averaging can improve upon the earlier attempts where the force constants were extracted empirically [17, 18] or from model inter-atomic potentials [27, 28] and thus,
- (iii) validate the combination of the TFC model and the ICPA as a reliable first-principles-based method for calculating the phonon spectra and related properties for disordered alloys which takes care of the microscopic aspects of various types of disorder.

We organize this paper as follows. Methodology and calculational details are presented briefly in section 2. We skip the details of the ICPA and the DFPT methodologies which are discussed earlier in the literature. Section 3 contains results and thorough discussions including experimental results as well as results obtained from our previous work on this alloy. Concluding remarks and future directions are presented in section 4.

2. Methodology and computational details

In the TFC approach, three assumptions are made to obtain the desired transferable properties. Only the nearest-neighbor interactions are considered because the longer-ranged force constants are ill-suited for the purpose. However, no serious error is expected to occur due to this because of the fact that, in the alloys considered, the distant-neighbor force constants are orders of magnitude smaller than the nearest-neighbor ones. The bending stiffnesses b are averaged over various spatial directions in order to obtain the effective isotropic bending stiffness and the off-diagonal terms in the force constant tensor Φ are constrained to be zero. Thus, the resulting force constant tensor has only two independent terms, the stretching stiffness s and the isotropic bending stiffness b :

$$\Phi(i, j) = \begin{pmatrix} b & 0 & 0 \\ 0 & b & 0 \\ 0 & 0 & s \end{pmatrix}.$$

Here the coordinate system is transformed such that the z axis is aligned along the direction connecting atoms i and j . This symmetrization ensures that the force constants never have a symmetry which is lower than the environment into which it is transferred. The dependence of s and b on the bond length l are transferable between different chemical environments. This dependence can be easily determined first by calculating the elements of the stretching–bending force constant tensor for a set of ordered structures so that enough dispersions of different bond distances are obtained and then by fitting these elements to an analytic function. To this end, we perform a set of calculations with different ordered structures at different compositions of FePd, each at different bond lengths. Taking our cue from van de Walle and Cedar [29], the force constant

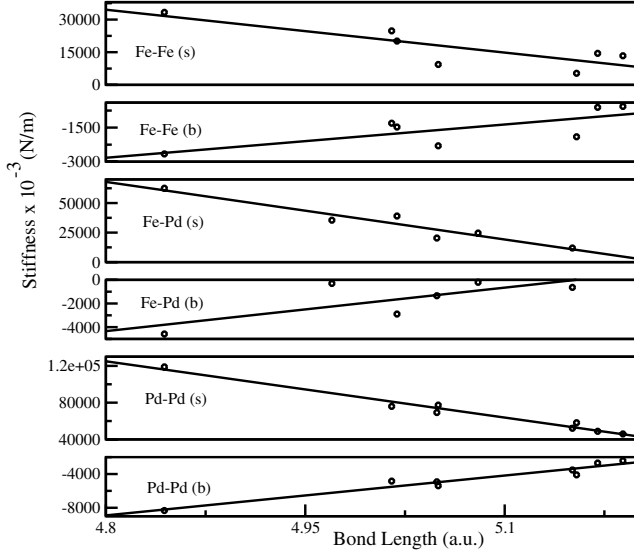


Figure 1. Nearest-neighbor stretching and bending force constants for $\text{Pd}_x\text{Fe}_{1-x}$ as a function of bond length. The solid lines are the fitted functions whereas the circles correspond to data obtained from *ab initio* calculations on a set of structures ($L1_2$ at four different volumes, $L1_0$ at two different volumes, and fcc Fe and fcc Pd at three different volumes).

versus bond distance data for each pair of chemical bonds is fitted using a linear relationship:

$$s(l) = s_0 + s_1(l - l_0) \quad (1)$$

$$b(l) = b_0 + b_1(l - l_0) \quad (2)$$

where l_0 is the equilibrium length of a particular bond and s_0, b_0 are the corresponding stiffness parameters. Once this is done, the inter-atomic force constants of any other structure can be determined solely from the knowledge of its equilibrium geometry.

First-principles Quantum-Espresso code [30], based upon a plane wave pseudopotential implementation of the DFPT, has been used to compute the Fe–Fe, Fe–Pd and Pd–Pd force constants at different bond lengths with different ordered structures. Force constants for L_{12} Fe_3Pd and FePd_3 , L_{10} FePd and fcc Fe and fcc Pd structures at their respective equilibrium and experimental lattice parameters have been used for construction of the transferable relation. Ultrasoft pseudopotentials [31] with nonlinear core corrections [32] were used. Perdew–Zunger parameterization of the local density approximation [33] were used for the exchange–correlation part of the potential. Plane waves with energies up to 55 Ryd are used in order to describe electron wavefunctions and Fourier components of the augmented charge density with cutoff energy up to 650 Ryd are taken into account. The Brillouin-zone integrations are carried out with Methfessel–Paxton smearing [34] using a $12 \times 12 \times 12$ \mathbf{k} -point mesh. The value of the smearing parameter is 0.02 Ryd. These parameters are found to yield phonon frequencies converged to within 5%.

After achieving the desired level of convergence for the electronic structure, the force constants are conveniently computed in reciprocal space on a finite \mathbf{q} -point grid and

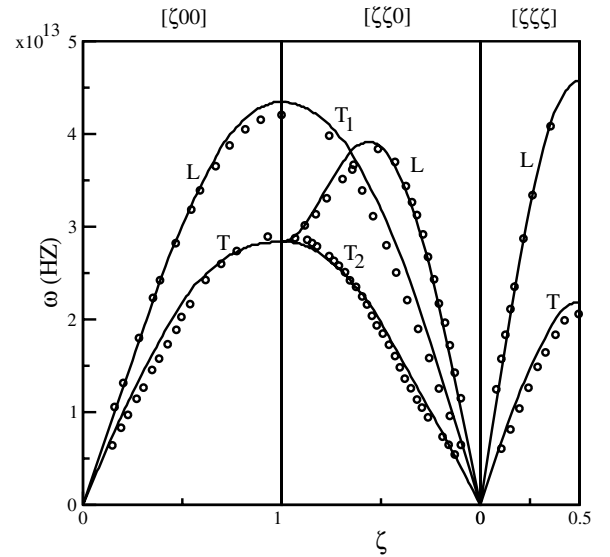


Figure 2. Dispersion curves (frequency ω versus reduced wavevector ζ): $\zeta = \frac{|\vec{q}|}{|\vec{q}_{\max}|}$, \vec{q} the phonon wavevector; for $\text{Pd}_{0.96}\text{Fe}_{0.04}$ calculated in the ICPA (solid lines) with the force constants obtained at the alloy bond length (5.189 au) using ‘bond stiffness versus bond length’ method. The circles are the experimental data.

Fourier transformation is employed to obtain the real-space force constants. The number of unique real-spaced force constants and their accuracy depend upon the density of the \mathbf{q} -point grids: the closer the \mathbf{q} -points are spaced, the more accurate the force constants are. In this work, we have used a $4 \times 4 \times 4$ \mathbf{q} -point mesh.

The required configuration averaging is performed by employing the ICPA method. The disorder in the force constants were considered for the nearest-neighboring shell only and the calculations were done on 400 energy points. A small imaginary frequency part of -0.05 was used in the Green’s functions. The Brillouin-zone integration was done over 356 \mathbf{q} -points in the irreducible Brillouin zone. The simplest linear-mixing scheme was used to accelerate the convergence. The number of iterations ranged from 5 to 15 for all the calculations. The phonon frequencies are obtained from the peaks of the coherent scattering structure factor defined as

$$\langle\langle S_\lambda(\vec{q}, w) \rangle\rangle_{\text{coh}} = \sum_{ss'} d_s d_{s'} \frac{1}{\pi} \text{Im} \langle\langle G_\lambda^{ss'}(\vec{q}, w^2) \rangle\rangle \quad (3)$$

where λ is the normal-mode branch index, d_s is the coherent scattering length for species s and $\langle\langle G_\lambda^{ss'}(\vec{q}, w^2) \rangle\rangle$ is the configuration-averaged spectral function associated with the species pair s, s' .

3. Results

Neutron-scattering results on phonon spectra for $\text{Pd}_{0.96}\text{Fe}_{0.04}$, $\text{Pd}_{0.9}\text{Fe}_{0.1}$ [35], $\text{Pd}_{0.5}\text{Fe}_{0.5}$ [36] and $\text{Pd}_{0.28}\text{Fe}_{0.72}$ [26] for all three symmetry directions are available along with the results on elastic constants. However, the measurements were done at different experimental conditions. While the measurements for

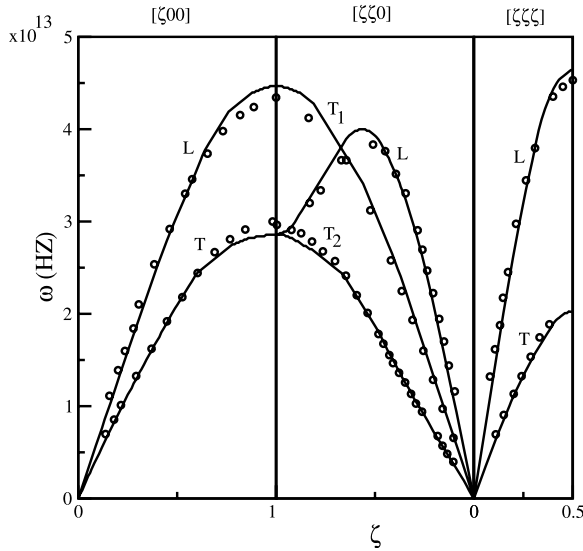


Figure 3. Dispersion curves (frequency ω versus reduced wavevector ζ): $\zeta = \frac{|\vec{q}|}{|\vec{q}_{\max}|}$, \vec{q} the phonon wavevector; for $\text{Pd}_{0.9}\text{Fe}_{0.1}$ calculated in the ICPA (solid lines) with the force constants obtained at the alloy bond length (5.17 au) using ‘bond stiffness versus bond length’ method. The circles are the experimental data.

$x = 0.96, 0.9$ and 0.28 (x is the Pd concentration) were done at room temperatures, the measurements for $x = 0.5$ were done at 1020 K. Accordingly, we discuss our results in two separate subsections.

3.1. $\text{Pd}_x\text{Fe}_{1-x}$ for $x = 0.96, 0.9$ and 0.28

The stretching and bending force constants for the alloy at the three concentrations are extracted from the fitted ‘bond stiffness versus bond distance’ relations as shown in figure 1. The curves in figure 1 show that the linear fitting is appropriate for the present case as the monotonic decrease of the force constants with the increasing bond distances is well captured for all three pairs of interatomic force constants. The computed values of correlation coefficient for the straight line fitting of stretching components of the force constant matrices varies between 0.83 and 0.99 which can be considered to be a very good fit. The fitting accuracy for the bending components is, however, a bit low with the calculated correlation coefficient varying between 0.74 and 0.97. But still, one can safely ignore this point as the bending components of force constant matrices are orders of magnitude smaller than the stretching components and therefore play minimal role in determining the phonon frequencies. The stretching and bending force constants for the three concentrations obtained from the fitted results are presented in table 1. The results show that for high Pd concentration systems, namely for $x = 0.96$ and 0.9 , the Fe–Fe and Fe–Pd force constants are softer by an order of magnitude than that of the Pd–Pd ones, with the Fe–Pd force constants being the softest. This is only to be expected because of the following reason: in a Pd-rich alloy like the ones discussed here, the Fe atoms would find lesser numbers of Fe atoms in the nearest-neighbor environment compared to that of the elemental Fe. As a result, the Fe–Fe and Fe–Pd interactions

Table 1. Computed force constants (in units of dyn cm^{-1}) for $\text{Pd}_x\text{Fe}_{1-x}$ using the TFC model. Results from other calculations [17, 18] are also presented for comparison.

Pair type	Conc. (x)	Bond length (au)	s (This work)	b (This work)	s (Other work)	b (Other work)
Fe–Fe	0.96	5.189	8 990	−930	13 366 ^a	−566 ^a
Pd–Pd	0.96	5.189	45 641	−2783	45 925 ^a	−2424 ^a
Fe–Pd	0.96	5.189	4 720	432	35 698 ^a	−1879 ^a
Fe–Fe	0.90	5.170	10 202	−1020	14 495 ^a	−609 ^a
Pd–Pd	0.90	5.170	49 404	−3073	48 768 ^a	−2699 ^a
Fe–Pd	0.90	5.170	7 718	206	36 272 ^a	−1992 ^a
Fe–Fe	0.28	5.019	20 157	−1760	—	—
Pd–Pd	0.28	5.019	80 323	−5457	—	—
Fe–Pd	0.28	5.019	32 345	−1655	—	—
Fe–Fe	0.50	5.12	13 573	−1271	—	—
Pd–Pd	0.50	5.12	59 874	−3880	—	—
Fe–Pd	0.50	5.12	16 057	−424	—	—
Fe–Fe	0.50	5.246	5 230	−651	15 400 ^b	−4100 ^b
Pd–Pd	0.50	5.246	33 983	−1883	41 800 ^b	−2900 ^b
Fe–Pd	0.50	5.07	24 136	−1035	30 600 ^b	−2500 ^b

^a Reference [18]. ^b Reference [17].

would be much softer compared to the Pd–Pd ones due to the overwhelming domination of the latter pair in the environment. In a recent paper [18], we tried to model the inter-atomic force constants for these two systems by calculating the Pd–Pd and Fe–Fe force constants in pure Pd and pure Fe lattices with the alloy lattice constant. The basic assumption behind such an approach was that the effect of environment on these force constants is expected to be less due to the high concentration of one of the constituents. The Fe–Pd interaction was modeled by hand adjustment starting from the concentration-averaged values. Although the results on the phonon spectrum had good agreement with the experiments, these choices were purely arbitrary and neglecting the environment effects limited its applicability for an arbitrary concentration. On the other hand, the TFC-based approach captures the effects of environment and thus leads to the correct understanding of the relative nature of interactions between different species pairs. A comparison of the results of the present calculation and those in [18] shows that the Pd–Pd force constants have near-perfect agreement while the Fe–Fe force constants are slightly stiffer in [18]. This definitely is an artifact of neglecting the role of environment. In the case of Fe–Pd force constants, we see a large difference. This is only to be expected, as in [18] the force constants were obtained by adjusting from concentration-averaged values based upon empirical observations and thus did not have a robust physical reasoning. On the other hand, the Fe–Pd interactions obtained by the TFC model have better reliability and accuracy because it is based upon the physical reality of transferability of the bond stiffness versus bond length relationship.

In the case of $\text{Pd}_{0.28}\text{Fe}_{0.72}$, the force constants obtained from the transferability relation as presented in table 1 show hardening of all three interatomic force constants in comparison to Pd-rich alloys. This behavior follows the expectation. Since the bond distances are smaller than the Pd-rich alloys, all three bonds were expected to stiffen. The Fe–Fe interactions harden because the Fe atoms can now find

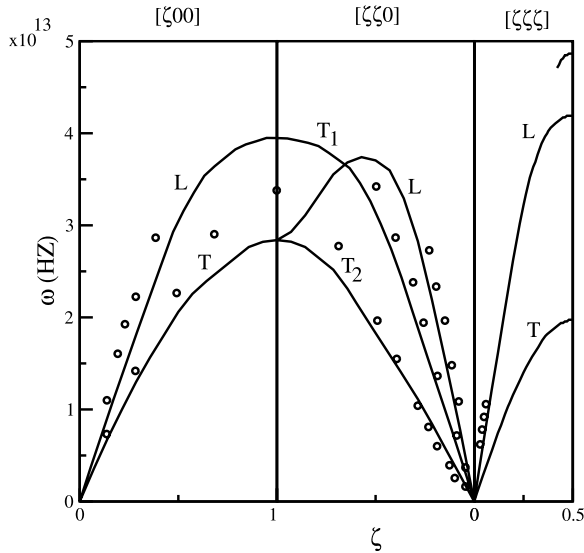


Figure 4. Dispersion curves (frequency ω versus reduced wavevector ζ): $\zeta = \frac{|\vec{q}|}{|\vec{q}_{\max}|}$, \vec{q} the phonon wavevector; for $\text{Pd}_{0.28}\text{Fe}_{0.72}$ calculated in the ICPA (solid lines) with the force constants obtained at the alloy bond length (5.019 au) using ‘bond stiffness versus bond length’ method. The circles are the experimental data.

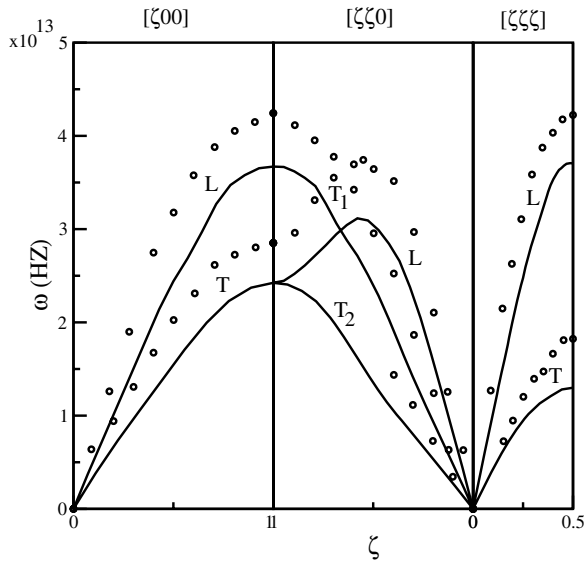


Figure 5. Dispersion curves (frequency ω versus reduced wavevector ζ): $\zeta = \frac{|\vec{q}|}{|\vec{q}_{\max}|}$, \vec{q} the phonon wavevector; for $\text{Pd}_{0.50}\text{Fe}_{0.50}$ calculated in the ICPA (solid lines) with the force constants obtained at the $L1_0$ bond length at 860 K (5.25 au for Fe–Fe and Pd–Pd and 5.07 au for Fe–Pd) using the ‘bond stiffness versus bond length’ method. The circles are the experimental data.

more Fe atoms in the neighboring environment. The Pd–Pd bonds stiffen because of the fact that the larger Pd atoms find themselves in a cage of smaller Fe atoms and the Fe–Pd interactions harden because of presence of more unlike pairs in the nearest-neighbor environment.

In what follows, we use the transferable force constants of table 1 as inputs to the ICPA and calculate the phonon dispersion curves for the three alloys. The phonon dispersion

Table 2. Computed elastic constants (in units of Mbar) for $\text{Pd}_x\text{Fe}_{1-x}$.

System	Elastic constant	Theo. (current paper)	Theo. ([18])	Expt. ([26, 35])
$\text{Pd}_{0.96}\text{Fe}_{0.04}$	C_{11}	2.17	1.97	2.3
	C_{12}	1.62	1.25	1.53
	C_{44}	1.09	1.26	0.78
$\text{Pd}_{0.90}\text{Fe}_{0.10}$	C_{11}	2.12	2.24	2.29
	C_{12}	1.59	1.41	1.65
	C_{44}	1.05	1.12	0.86
$\text{Pd}_{0.28}\text{Fe}_{0.72}$	C_{11}	1.50	—	1.40 ± 0.20
	C_{12}	1.13	—	1.34 ± 0.18
	C_{44}	0.75	—	0.80 ± 0.02

curves for $\text{Pd}_{0.96}\text{Fe}_{0.04}$, $\text{Pd}_{0.9}\text{Fe}_{0.1}$ and $\text{Pd}_{0.28}\text{Fe}_{0.72}$ calculated with these sets of force constants are presented in figures 2, 3 and 4, respectively. It can be seen that calculated and experimental results of phonon frequencies for $\text{Pd}_{0.96}\text{Fe}_{0.04}$ and $\text{Pd}_{0.9}\text{Fe}_{0.1}$ alloys are in excellent agreement for all the symmetry directions. The calculated phonon frequencies of the $\text{Pd}_{0.28}\text{Fe}_{0.72}$ alloy also agree reasonably well with experimental values except near the zone edges. This disagreement could be because of using the LDA as the exchange–correlation functional at the experimental lattice constant for a Fe-rich system. Earlier calculations with pure Fe [37] had shown that the calculated frequencies are underestimated if one uses the LDA at the experimental lattice constant which is larger than the LDA equilibrium lattice constant. Another noteworthy feature in the dispersion curves for $\text{Pd}_{0.28}\text{Fe}_{0.72}$ is that, near the zone edge, a splitting in the dispersion curves is observed in the longitudinal branch along the $[\zeta, \zeta, \zeta]$ direction. This kind of splitting in the dispersion curves is a typical feature of strong force constant disorder and is seen in the past for some other alloys too [10]. However, experimental data for high wavevectors are not available for confirmation.

The overall results, therefore, show that the phonon frequencies calculated by a combination of the TFC model and the ICPA agree well with the experimental results for both Pd-rich and Fe-rich alloys. To further validate the approach, we present results for elastic constants in table 2. A comparison with the experimental results and our earlier calculations with empirical force constants is also done. The results show an overall improvement of all the elastic constants calculated in the present approach as compared to the approach with empirical force constants for $\text{Pd}_{0.96}\text{Fe}_{0.04}$ and $\text{Pd}_{0.9}\text{Fe}_{0.1}$. The calculated elastic constants for $\text{Pd}_{0.28}\text{Fe}_{0.72}$ have excellent agreement with experimental results as well.

3.2. $\text{Pd}_{0.5}\text{Fe}_{0.5}$

The system $\text{Pd}_{0.5}\text{Fe}_{0.5}$ needs separate attention from the point of view of comparison between experimental and theoretical results. This is because of the fact that, unlike the other systems considered so far, neutron-scattering measurements on this system were done at a high temperature. It would, therefore, be interesting to see how far the present TFC model can address the complex interplay of interatomic forces between various species pairs since the construction of the TFC model did

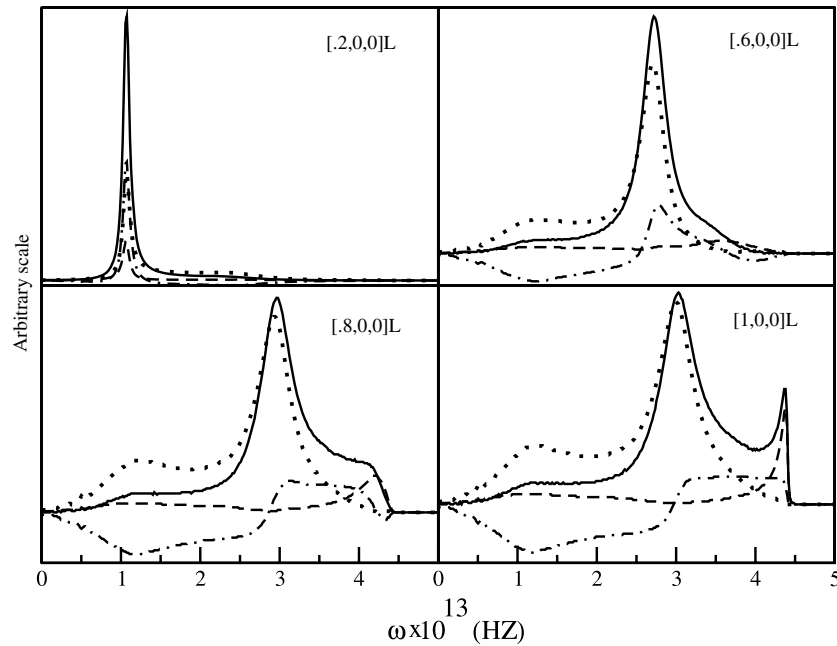


Figure 6. Partial and total structure factors calculated by the ICPA for various ζ values in the $[\zeta, 0, 0]$ direction in $\text{Pd}_{0.50}\text{Fe}_{0.50}$ using the force constants extracted at the disordered alloy bond length (5.12 au). The solid lines are the total contributions, the dotted lines are the Fe–Fe contributions, the long-dashed lines are the Pd–Pd contributions and the dotted–dashed lines are the Fe–Pd contributions. All the curves are for longitudinal modes.

not take care of temperature effects. As is done in the cases for the alloys at other compositions we calculate the phonon frequencies by the ICPA using the force constants extracted at the disordered alloy bond length (5.12 au). To understand the contributions of each pair of species towards the normal modes, we look into the partial and the average structure factors. In figure 6, we present results for the structure factors along the $[\zeta, 0, 0]$ direction and for the longitudinal branch at some selected ζ values. No anomalous behavior is observed for low and medium wavevectors for which single distinct peaks in the structure factors are observed. However, for $[0.8, 0, 0]$ an additional peak begins to appear which is clearly visible at $[1, 0, 0]$. This, in turn, means that there would be the existence of a split branch along the particular direction in the frequency spectrum. The partial structure factors show that the spurious high frequency peak is due to the Pd–Pd pairs and, to a smaller extent, due to Fe–Pd pairs. As is mentioned already, the splitting of the high frequency branch is a typical feature of strong force constant disorder and has been reported for some alloys. To understand its origin, we look at the force constants from table 1. It is observed that the Fe–Fe and Fe–Pd force constants differ significantly from Pd–Pd force constants, thereby representing a situation of very strong disorder. We can, therefore, conclude that the strong force constant disorder causes the splitting of the high frequency branch. Since the experimental results [36] do not show any such splitting, these force constants do not represent the correct picture of the microscopic interactions in $\text{Pd}_{0.50}\text{Fe}_{0.50}$.

In [36] neutron-scattering experiments were done on ordered L1_0 FePd at room temperature and at a temperature close to the order–disorder transition. The force constants in the L1_0 structures at those temperatures were also extracted

by fitting the measured frequencies to a Born–Von Karman model. In [17], one of us used the experimental force constants for L1_0 structure at 860 K, a temperature close to the order–disorder transition temperature 950 K, as the disordered alloy force constants in the ICPA calculations and obtained excellent agreement with experiments. It was, therefore, argued that the force constants at 860 K correctly represent the ones of the disordered alloy because of the fact that, near the order–disorder transition temperature, the ordered and disordered states are expected to be in perfect equilibrium, with the disordered state possessing short-range order. To see whether this was indeed the case, we next use the interatomic bond distances of various pairs in the L1_0 structure at 860 K to extract the fitted force constants. The results along with the ones used in [17] are presented in table 1. It is observed that the Fe–Fe and Pd–Pd bonds soften in comparison to the ones at disordered alloy bond distances, with the Pd–Pd being mostly affected. The Fe–Pd bonds harden because of the shortening of the corresponding bond distances. However, all the bonds are significantly softer than the ones in [17]. To see whether the fitting to the L1_0 bond distances get rid of the spurious peak in the structure factors of figure 6 and thus wash away the split-peak behavior, we plot the structure factors for the $[1\ 0\ 0]$ longitudinal branch in figure 7. Unlike the previous structure factors (figure 6), no dual-peak structures appear in this case. The single high frequency peak is now mostly because of the Fe–Pd contribution; the Fe–Fe and Pd–Pd contributions only add more weights to the single peak. This signifies that Pd–Pd contributions were overestimated whereas the Fe–Pd contributions were grossly underestimated by the calculations at the disordered bond length. The corresponding dispersion curves are presented in figure 5. The results suggest

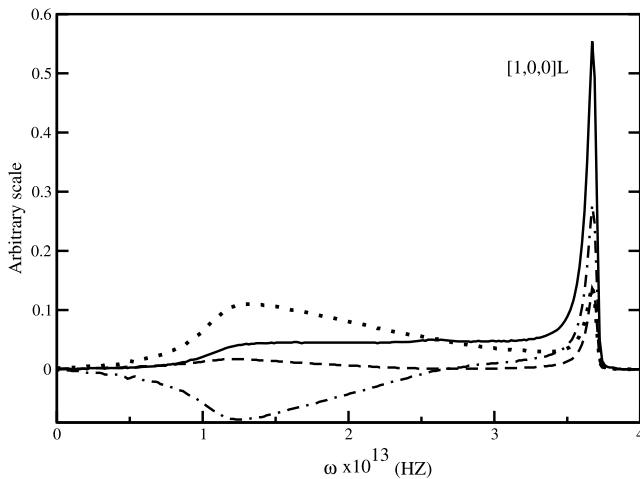


Figure 7. Partial and total structure factors calculated by the ICPA for $\zeta = 1$ in the $[\zeta, 0, 0]$ direction in $\text{Pd}_{0.5}\text{Fe}_{0.5}$ with force constants calculated at the $L1_0$ bond lengths. The solid lines are the total contributions, the dotted lines are the Fe–Fe contributions, the long-dashed lines are the Pd–Pd contributions and the dotted–dashed lines are the Fe–Pd contributions. All the curves are for longitudinal modes.

that the consideration of the $L1_0$ bond distances produce the correct qualitative features as we do not see any peak splitting. Thus, the results *a posteriori* validate the approximation with reference to interatomic force constants in [17]. However, the qualitative agreement with the experimental results is far from satisfactory. The calculated frequencies are significantly underestimated in this case. This is a reflection of overall softening of the force constants as discussed above. The reason for this underestimation could be because of the non-incorporation of any temperature effect in the fitting model. This incorporation, however, is a non-trivial task and is beyond the scope of the present context.

4. Conclusions

A combination of the transferable force constant model based upon first-principles calculations and the ICPA has been proposed as a first-principles-based tool to calculate the phonon spectrum and related properties for disordered alloys at any arbitrary concentration. The TFC model, for the first time, is applied to calculate the complete phonon spectra of disordered alloys. The reliability of the model is also examined in the context of magnetic type-II alloys. The phonon dispersion curves and elastic constants for $\text{Pd}_x\text{Fe}_{1-x}$ alloys agree very well with the experiments at low temperatures. For $\text{Pd}_{0.5}\text{Fe}_{0.5}$ alloys, the qualitative features of the various inter-atomic force constants are also well reproduced with this approach. The deviation of the calculated phonon frequencies from the experimental results could be attributed to the non-incorporation of any temperature effect in calculating the force constants. The combination of the TFC and the ICPA, thus, can be considered as an accurate first-principles-based methodology for calculating lattice dynamics for disordered alloys and can stand out as an answer to the long-standing problem in this area of research.

Acknowledgment

One of the authors (BD) would like to acknowledge CSIR, India for financial support under grant-F.No:09/731(0049)/2007-EMR-I.

References

- [1] Bruesch P 1982 *Phonon, Theory and Experiment* (New York: Springer)
- [2] Bogdanoff P D, Fultz B and Rosenkranz S 1999 *Phys. Rev. B* **60** 3976
- [3] Fultz B, Anthony L, Robertson J L, Nicklow R M, Spooner S and Nostoller M 1995 *Phys. Rev. B* **52** 3280
- [4] Swan-Wood T L, Delaire O and Fultz B 2005 *Phys. Rev. B* **72** 024305
- [5] Bogdanoff P D, Swan-Wood T L and Fultz B 2003 *Phys. Rev. B* **68** 014301
- [6] Anthony L, Nagel L J, Okamoto J K and Fultz B 1994 *Phys. Rev. Lett.* **73** 3034
- [7] Fultz B, Stephens T A, Sturhahn W, Toellner T S and Alp E E 1998 *Phys. Rev. Lett.* **80** 3304
- [8] Kentzinger E, Cadeville M C, Pierron-Bohnes V, Petry W and Hennion B 1996 *J. Phys.: Condens. Matter* **8** 5535
- [9] Robertson I M 1991 *J. Phys.: Condens. Matter* **3** 8181
- [10] Ghosh S, Leath P L and Cohen M H 2002 *Phys. Rev. B* **66** 214206
- [11] Hohenberg P and Kohn W 1964 *Phys. Rev.* **136** B864
- [12] Kohn W and Sham L J 1965 *Phys. Rev.* **140** A1133
- [13] Baroni S, De Gironcoli S, Dal Corso A and Giannozzi P 2001 *Rev. Mod. Phys.* **73** 515
- [14] Mookerjee A 1973 *J. Phys. C: Solid State Phys.* **6** L205
- [15] Taylor D W 1967 *Phys. Rev.* **156** 1017
- [16] Ghosh S, Neaton J B, Antons A H, Cohen M H and Leath P L 2004 *Phys. Rev. B* **70** 024206
- [17] Alam A, Ghosh S and Mookerjee A 2007 *Phys. Rev. B* **75** 134202
- [18] Dutta B and Ghosh S 2009 *J. Phys.: Condens. Matter* **21** 095411
- [19] Sanchez J M, Ducastelle F and Gratias D 1984 *Physica A* **128** 334
- [20] Sluiter M H, Weinert M and Kawazoe Y 1999 *Phys. Rev. B* **59** 4100
- [21] van de Walle A and Ceder G 2000 *Phys. Rev. B* **61** 5972
- [22] van de Walle A 2000 *PhD Thesis* MIT, Cambridge
- [23] Wu E J, Ceder G and van de Walle A 2003 *Phys. Rev. B* **67** 134103
- [24] Liu J Z, Ghosh G, van de Walle A and Asta M 2007 *Phys. Rev. B* **75** 104117
- [25] Noda Y and Endoh Y 1988 *J. Phys. Soc. Japan* **57** 4225
- [26] Sato M, Grier B H, Shapiro S M and Miyajima H 1982 *J. Phys. F: Met. Phys.* **12** 2117
- [27] Singh N 1990 *Phys. Rev. B* **42** 8882
- [28] Akgun I and Ugur G 1995 *Phys. Rev. B* **51** 3458
- [29] van de Walle A and Ceder G 2002 *Rev. Mod. Phys.* **74** 11
- [30] Quantum-Espresso is a community project for high-quality quantum-simulation software, based on density functional theory, and coordinated by P Giannozzi See <http://www.Quantum-Espresso.org/> and <http://www.pwscf.org>
- [31] Vanderbilt D 1990 *Phys. Rev. B* **41** 7892
- [32] Louie S G, Froyen S and Cohen M L 1982 *Phys. Rev. B* **26** 1738
- [33] Perdew J P and Zunger A 1981 *Phys. Rev. B* **23** 5048
- [34] Methfessel M and Paxton A T 1989 *Phys. Rev. B* **40** 3616
- [35] Maliszewski E, Sosnowski J, Bednarski S, Czachor A and Holas A 1975 *J. Phys. F: Met. Phys.* **5** 1455
- [36] Mehaddene T, Kentzinger E, Hennion B, Tanaka K, Numakura H, Marty A, Parasote V, Cadeville M C, Zemirli M and Pierron-Bohnes V 2004 *Phys. Rev. B* **69** 024304
- [37] Dal Corso A and De Gironcoli S 2000 *Phys. Rev. B* **62** 273